Compressor Surge and Stall Propagation[1]

By H. W. EMMONS,[2] C. E. PEARSON,[3] AND H. P. GRANT,[3] CAMBRIDGE, MASS.

Compressor surge is shown by the application of several types of instrumentation (notably a hot-wire anemometer) to consist of two distinct types of phenomena. The whole compressor flow system may be unstable in the manner of a self-excited Helmholtz resonator. The theory of this instability is presented and is shown to explain some of the observed pulsation symptoms. The stalling of the flow through the blade rows, which usually is assumed to be the origin of pulsation, is shown to occur in propagating groups of 1 to 5 regions involving from 2 to 20 blades each. The theory of this "stall propagation" shows the propagation velocity relative to the wheel to be dependent upon boundary-layer growth parameters and hence the frequency (relative to a stationary probe) to be proportional to the wheel speed. Another part of observed compressor pulsation thus is explained. These two phenomena frequently interact to produce complex performance characteristics. The theories presented are essentially correct as shown by experimental verification, but much remains to be done to make quantitative compressor-performance prediction practical.

Introduction

IN THE long run, the successful prediction of the performance of a bladed compressor requires a qualitative knowledge of the flow behavior likely to be encountered in the machine and adequately quantitative mathematical methods for describing the behavior in terms of accurately measurable quantities.

In a small and useful area of the possible range of design and operating parameters of a multistage axial-flow machine (closely spaced blades, low air-incidence angles, low air-turning angles, large hub-tip ratio, small inlet boundary-layer thickness), both these requirements have been met. The flow has been observed experimentally to be nearly two-dimensional (small radial flow) and steady, and the mathematics describing viscous compressible flow under these conditions has been made manageable.

In other areas, however, prediction of performance has not been noticeably successful as yet. The demand for a fuller understanding is perhaps most pressing in the high-angle-of-incidence low-flow regime of compressor operation. Here, violent over-all instabilities identified with the generic term "surge" most often have been reported, typical symptoms being audible thumping and honking at inlet and exit (at frequencies as low as 1 cycle per sec [cps]), severe mechanical vibration, and oscillation of recorded pressures throughout the machine.

Violent surge cannot be tolerated in an aircraft gas turbine since there is obvious danger of mechanical failure or interruption of the combustion process; but if the machine is to start without elaborate auxiliary equipment and if it is to operate during the sudden accelerations and rapid changes in inlet conditions encountered in highly maneuverable aircraft, then the compressor occasionally must operate at low flow rates and high incidence angles. The problem of predicting and controlling surge behavior is clearly an important one and is becoming increasingly important as size and rotational speeds of engines steadily increase.

Experimental evidence has been vague and conflicting (partly because of the limitations of conventional instrumentation). Of the surge frequencies which have been reported, some have varied with the speed of the machine and others have not. Volume of connected ducting affected the violence and frequency of surge in some reported cases and did not in others. (Examples will be given later.) That no successful analysis or prediction of surge behavior has been reported previously is not surprising, since what sketchy qualitative information was available indicated only that no single simple flow phenomenon was responsible. It seemed that there well could exist several modes of instability, and that the variety of surge symptoms reported was due to the occurrence of various combinations of them in any one machine. These ideas could remain only in the realm of speculation until more indicative experimental evidence became available.

It now can be reported that new evidence has been obtained by applying a hot-wire instrument developed at Harvard (1)[4] to a thorough study of velocity and pressure fluctuations in a centrifugal compressor with a rotating axial-flow inducer blade row, and in a single-stage axial machine. Each had shown previously its own set of surge symptoms in the low-flow operating range. The hot-wire investigations indicated that two distinct phenomena predominated, one a Helmholtz "organ-pipe" resonance in the larger chambers of the machines, and the other a particular form of blade-row flow instability characterized by the propagation of blade stall from blade to blade along the axial-flow rows in the direction of relative inlet tangential velocity. Both phenomena were present in both machines, and either could produce certain external symptoms of "surge"; between them they accounted for all observed symptoms. Phenomenologically sound theoretical explanations could be found for each, and though at present the analyses hardly could be termed adequately quantitative, criteria for the onset of surge symptoms and methods for avoiding them can be suggested, and the most hopeful direction for further investigation can be indicated.

We shall consider in Section 1 the initial experimental observations, and in Sections 2 and 3 the analyses of the two flow phenomena, together with additional experimental checks.

1 EXPERIMENTAL INVESTIGATION OF SURGE IN TWO COMPRESSOR-TEST RIGS

Introductory Remarks

During extensive conventional performance testing in the two machines to be described, operators had reported symptoms of unstable flow behavior in a variety of operating regions. This information was supplemented at an early date by some records of low-frequency wall static-pressure fluctuation at points of interest along the flow path in each machine. These observations

[1] The results presented in this paper form a portion of recent research supported by Pratt and Whitney Aircraft, to whom the authors are indebted for permission to publish the paper.

[2] Professor of Engineering Sciences, Department of Engineering Sciences and Applied Physics, Harvard University. Mem. ASME.

[3] Harvard University.

Contributed by the Gas Turbine Power Division and presented at a joint meeting of the Gas Turbine Power and Hydraulic Divisions at the Annual Meeting, New York, N. Y., November 29–December 4, 1953, of THE AMERICAN SOCIETY OF MECHANICAL ENGINEERS.

NOTE: Statements and opinions advanced in papers are to be understood as individual expressions of their authors and not those of the Society. Manuscript received at ASME Headquarters, September 9, 1952. Paper No. 53—A-65.

[4] Numbers in parentheses refer to Bibliography at end of paper.

will be examined briefly, for they are typical of the information commonly available to engineers concerned with the surge problem. The results of a detailed qualitative study of velocity fluctuations within the two machines, carried out with the hot-wire instrument of reference (1), then will be considered.

Nomenclature used in this section is as follows:

- a = local speed of sound, fps
- i = air incidence angle (relative to tangent to mean camber line at leading edge), deg
- p_t = area-average total pressure, psf
- A = area, sq ft
- U = rotor-tip speed, fps
- W = weight flow, lb per sec
- ρ = air density, pcf
- $()_1$ = condition ahead of compressor
- $()_2$ = condition well behind compressor

Test Stands

The two test rigs are of widely different physical characteristics. The single-stage axial stand was designed to avoid extensive ducting in series with the compressor. Laboratory air is drawn through a short annular elbow directly into a test section containing rotor and stator, and exhausted immediately back into the room through a movable cone throttling diffuser.

The centrifugal test stand was designed to throttle at either inlet or exit and to discharge outside the building; these features required a large chamber containing calming screens and straighteners between the inlet throttling (butterfly) valves and the test section, and some 40 ft of ducting and valves at the exit. The test section itself contains an axial-flow inducer-blade row and a straight-radial-bladed centrifugal impeller followed by a vaneless radial diffuser and collector case.

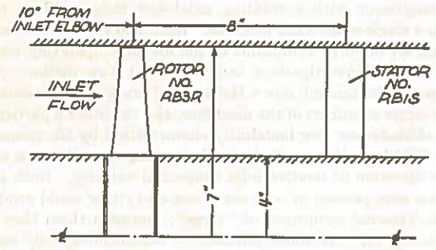

Fig. 1 Axial-Flow Compressor Stage

Several stages were tested in the single-stage axial machine and all showed similar surge symptoms. The rotor-stator combination in Fig. 1 was studied in greatest detail. It has characteristics typical of early stages in a multirow axial-flow machine, i.e., fairly low hub-tip ratio, high gap-chord ratio (1.7 at mean radius), and moderate turning (rotor-blade camber angle 30 deg at mean radius).

All testing in the centrifugal stand was carried out on the single inducer-impeller-diffuser combination shown in Fig. 2 whose principal physical characteristics are low inducer hub-tip ratio, large inducer camber angle (60 deg), and moderate impeller hub-tip ratio.[5]

Over-All Performance Tests

Curves of total-pressure ratio versus flow for each machine are

[5] The inducer and impeller of this centrifugal compressor were matched badly. It should be mentioned that both the axial and centrifugal test stages were old experimental designs.

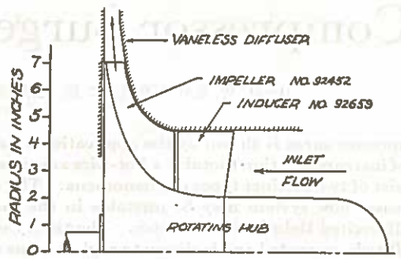

Fig. 2 Centrifugal Test Rotor

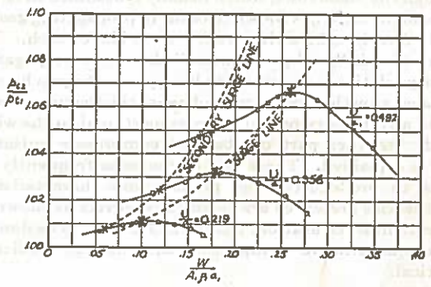

Fig. 3 Axial Compressor Pressure Ratio Versus Mass-Flow Factor

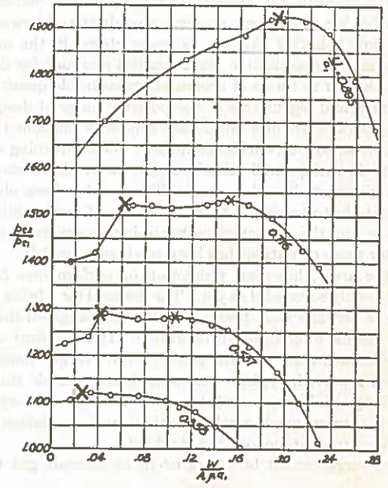

Fig. 4 Centrifugal Compressor Pressure Ratio Versus Mass-Flow Factor

shown in Figs. 3 and 4. This information was recorded during conventional survey programs in which flow was varied by exit throttling at each of a series of rotor speeds in the low-speed range where violence of surge was not excessive. Instrumentation consisted of arrays of fixed probes well ahead of and well behind the compressors. Flow was metered by a previous calibration of inlet-passage-wall static taps in each machine.

It can be observed from Figs. 3 and 4 that a variety of pressure-rise-curve shapes were encountered. The axial compressor yielded

smoothly humped curves at all speeds, while the centrifugal machine produced characteristics of three distinct shapes, including (*a*) at lowest speeds, a smoothly rising pressure ratio from maximum flow to nearly zero flow, with sudden drop there, (*b*) at high speed, a double peaked characteristic, (*c*) at high speeds, a curve peaking near maximum flow and falling smoothly between that point and zero flow.

Surge points reported at various times are marked with heavy crosses in Figs. 3 and 4. In the axial-stand tests, all operators agreed that noise level increased sharply and recorded pressures tended to become unstable at the peak of the performance curve at each speed, although no predominant frequency of audible noise was reported. The locus of these points was designated the surge line of the compressor. It was noticed that at a somewhat lower flow rate at each rotor speed, low frequencies (less than 100 cps) that varied with rotor speed became distinct, and pressures read at upstream wall static taps rose slightly, suggesting local flow redistribution. The locus of these points was designated the "secondary surge line." As the exit throttle was closed further, noise level diminished steadily, until at zero flow operation was quiet and, to all appearances, stable. Upon reopening the exit valve the sequence was repeated in reverse, with a slight hysteresis behavior in static pressures reported in the vicinity of the secondary surge line.[6]

In the centrifugal stand tests, the reports of surge behavior were particularly confusing; as flow was decreased at any fixed rotor speed, a point eventually was reached at which a violent thumping (at about 10 cps at all speeds) became evident. Mechanical vibration became severe and pressures read at upstream wall static taps rose well above inlet total pressure. At the lower speeds this point coincided with the sharp drop in pressure ratio near zero flow; at higher speeds it occurred with the gradual drop in total pressure ratio from the peak value near maximum flow. In addition, at intermediate speeds, some operators reported sharp increases in noise level at the points indicated by the lighter crosses, although the 10-cps frequency was not distinctly audible.

Pressure-Fluctuation Observations

Measurements of low-frequency pressure fluctuations were made at various stations along the casing of each machine by the simple hot-wire technique diagrammed in Fig. 5. A hot-wire

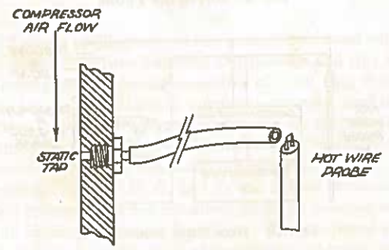

Fig. 5 Instrumentation for Low-Frequency Pressure-Fluctuation Measurements

probe (of the type shown later in Fig. 9) is held at the open end of a length of plastic tubing leading from a wall static tap. Static-pressure fluctuations show up as oscillations in the velocity of air of the tubing; the resultant fluctuations in the voltage across the wire (operated at constant heating current) are amplified and

[6] When the exit valve was opened very carefully from the completely closed position, steady over-all backflow through the entire machine sometimes could be obtained.

presented on an oscilloscope for examination. High frequencies are damped out by the use of a 10-ft piece of tubing. This instrument provides a good quantitative measure of surge frequency and a qualitative picture of violence of surge.

The results of these surveys are shown in Figs. 6 and 7. When flow is reduced at constant rotor speed corresponding to U/a_1 =

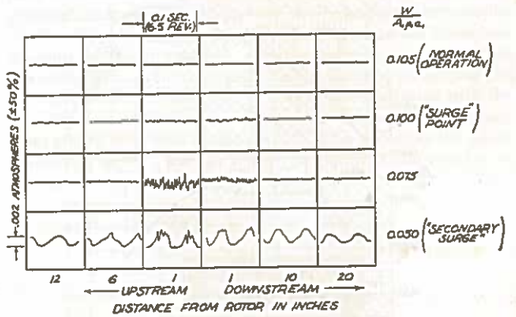

Fig. 6 Pressure Fluctuations in the Axial Test Stand; $U/a_1 = 0.219$

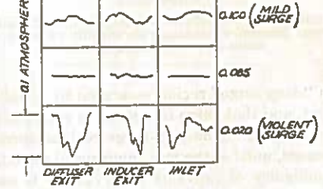

Fig. 7 Pressure Fluctuations in Centrifugal Test Stand; $U/a_1 = 0.537$

0.219 in the axial compressor, Fig. 6, the flow becomes noticeably rough in the vicinity of the rotor as the surge line is crossed, although flow a few inches either side of the rotor remains fairly smooth. Shortly before the secondary surge line is reached, a large 200-cps pressure fluctuation becomes predominant in the vicinity of the rotor; pressure fluctuations elsewhere are still negligible. At the secondary surge line, an enormous 20-cps pressure pulse appears abruptly throughout the machine, with maximum amplitude near the rotor, but dying in amplitude only slightly upstream and downstream. Similar tests at other rotor speeds with this stage showed identical behavior, except that the frequencies encountered just before secondary surge and in secondary surge varied almost directly with rotor speed. This behavior defied analysis; clearly the acoustic dimensions of the machine were not the controlling factor, and thus the most convenient explanation of surge behavior was eliminated.

In the centrifugal stand, Fig. 7, a similar set of measurements revealed a different behavior. It became evident that at the rotor speed tested there existed two clearly defined surge regions (in which low-frequency pulsing occurred throughout the machine) separated by a region of stable operation (in the sense that no low-frequency pulsing was observed anywhere in the machine). In the first surge region the predominant frequency was 10.5 cps;

in the second, more violent, surge region near zero flow, the predominant frequency was 9.5 cps. The series of inlet-pressure fluctuation tests, summarized in Fig. 8, were run subsequently to define pulsating-flow regions throughout the operating range of this test stand. At low rotor speeds, note that there is a "mild

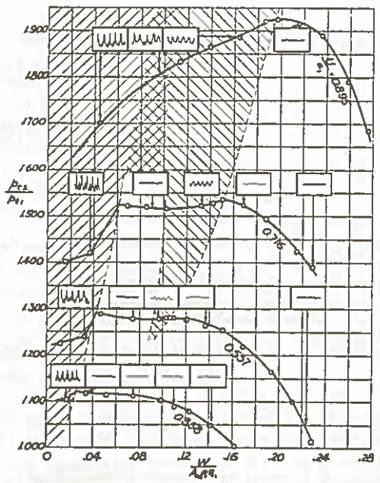

Fig. 8 Surge Regions in Operating Range of Centrifugal Compressor

(As shown by inlet pressure-fluctuation oscillograms; each oscillogram shows one 1/2-sec sweep; pressure fluctuations are roughly to scale; shading indicates extent of surge regions.)

surge" and a "deep surge" region separated by a stable range, as in the first test, and that surge frequency in each region is nearly independent of speed. The two surge regions spread as rotor speed is increased, until at the maximum speed tested, they overlap. The ambiguity of previous observations is easily understood.

Hot-Wire Velocity-Fluctuation Surveys

The underlying causes of these various compressor-surge symptoms became clear with the application of the constant-current hot-wire instrument developed at Harvard (1). The hot-wire principle is familiar. The electrical resistance of a metal varies with its temperature; therefore, when a tiny electrically heated tungsten wire (operating at constant heating current) is exposed to a cooling-air stream of known temperature, the average voltage across the wire becomes a measure of the component of average stream velocity which is perpendicular to the wire (that component being, in general, the only one effective in cooling a thin wire). It was shown (1) that when the heated wire is exposed to large and rapid velocity fluctuations, the magnitude of the instantaneous time derivative of the resulting fluctuating voltage across the wire is a direct measure of the instantaneous velocity perpendicular to the wire.

For precise measurement of instantaneous velocity, a careful calibration of each wire is required,[7] and a fairly accurate record of air temperature and "cold-wire" resistance during subsequent tests must be kept. For qualitative work, simplification is possible, since over a wide range of operation the relation between instantaneous velocity and time derivative of wire voltage is nearly linear, and the constant of proportionality is affected only slightly by large changes in air temperature or even by large collections of dirt on the wire. A record of voltage time derivative versus time is obtained easily using conventional oscillographic techniques, so a rapid qualitative survey of velocity fluctuation with a precision of about ±20 per cent is relatively simple. Calibration of each wire is unnecessary; the scale factor between oscilloscope deflection and velocity fluctuation is obtained easily by placing each new wire at a standard reference point where the velocity fluctuation is known. This procedure is sufficiently accurate for the purpose of qualitative surveys, such as are presented here.

The hot-wire probe used in the present investigation is a modification of that described in reference (1), a sketch of which is shown in Fig. 9. A length of tungsten wire is supported by two tapered steel needles fixed in a lucite insert pressed into the end of a steel tube. Current-carrying leads soldered to the needles lead through the tube to a battery supply. The complete electric circuit is shown in Fig. 10; a large resistor in series with the

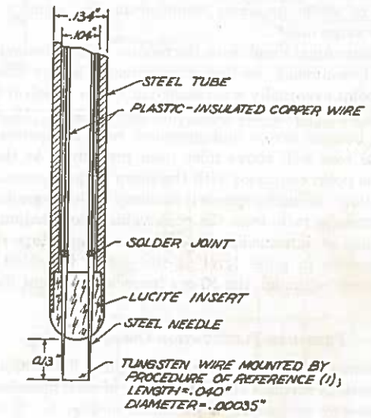

Fig. 9 Hot-Wire Probe

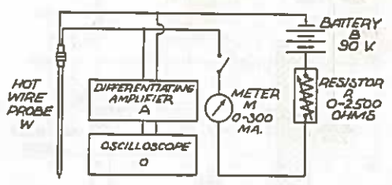

Fig. 10 Hot-Wire Instrument

hot wire renders its current almost independent of its resistance. The derivative of the voltage across the hot wire is amplified by A, and presented on an oscilloscope screen O. As a matter of practical interest, it may be mentioned that the source of most hot-wire difficulties is the tungsten-steel connection. It is necessary that very careful copperplating and soldering techniques be employed. With experience, wires with a useful life of over 100 hr of operation may be constructed. Occasionally it is necessary to clean off the film of thick sludge which gradually accumulates on the wire because of the presence of oil in the air.

[7] A wire needs to be calibrated only once in its lifetime. The simple correction method of reference (1) compensates for changes in wire characteristics due to plastic flow, oxidation, change in steel-copper-tungsten contact resistance, etc.

Experimental Results

In general, flow behavior was examined in both machines at all points accessible to a probe. The most interesting results were obtained close behind the axial-flow blade rows in each stand. The behavior of the axial component of velocity at inducer exit in the centrifugal stand was perhaps the most spectacular and will be considered first.

In general, with the wire perpendicular to the rig axis and close behind the rotating inducer, we would expect to see velocity patterns similar to those obtained in pressure traverses behind a stationary cascade. Fig. 11 shows typical cascade exit-velocity profiles over a wide range of incidence angles and indicates the predicted shapes of differentiated hot-wire signals behind a rapidly moving cascade over a similar incidence range. The hot wire should depart from the correct velocity profile only under conditions of reverse flow (since the wire does not distinguish sense of flow). Some clipping of sharp velocity maxima and minima might be expected because of the finite length of the wire.

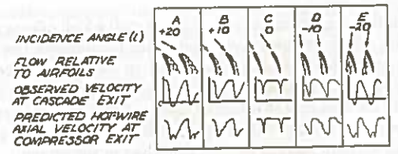

Fig. 11 Predicted Hot-Wire Response

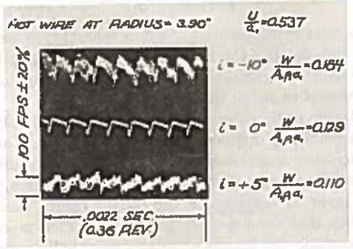

Fig. 12 Oscillograms of Axial Velocity Fluctuations at Exit of Inducer-Blade Row

Fig. 12 shows oscillograms of the inducer-exit axial velocity at a radial position midway between mid-passage and tip; the flow points correspond to incidence angles of —10 deg, 0 deg, and +5 deg, i.e., to conditions of maximum, normal, and incipient surge flows. Several traces are superposed on each oscillogram. Since time goes from left to right, and velocity increases upward, the distributions can be compared directly with those of Fig. 11. The predicted profiles B, C, and D are indeed obtained. The predicted profile E was not obtained, probably because of the inability to obtain sufficiently high flow. The predicted profile A was not observed clearly, since an instability behavior developed at about an incidence angle of 6 deg, that is, at a flow point slightly removed from the surge point. Fig. 13 shows the typical flow behavior encountered at this point; groups of stalled blades and groups of unstalled blades passed the hot wire alternately in a periodic pattern. The possibilities are now twofold; either the entire rotor stalls and unstalls periodically as a unit, or cells of stall are present on the wheel and rotate around it in time (relative to a stationary system). Since the pattern of Fig. 13 was obtained at all circumferential positions, the possibility of intermittent stall in a local region need not be considered. The frequency with which the stall cells appeared was not an integral multiple of rotor frequency, thus eliminating the possibility of stall cells fixed to the wheel.

To investigate the behavior further, the hot-wire instrument diagrammed in Fig. 14 was constructed; the existence of the two channels now permitted simultaneous measurements at various pairs of points. It was found that there were three cells of stall propagating around the wheel, each involving about three stalled blades. The direction of propagation relative to the wheel was opposite to wheel rotation, and the velocity of propagation was about 0.75 that of the wheel; that is, the cells moved past the hot wire in the same direction as that of wheel rotation with the velocity of about 0.25 that of the wheel. It also was found that these stalled cells were wedge-shaped, being widest at the tip as shown in Fig. 15. Further study revealed that the velocity of propagation varied directly with wheel speed.

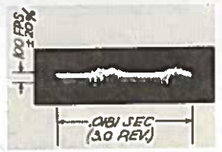

Radius = 3.90 in. $\frac{U}{a_1} = 0.537$

$i = +6$ deg $\frac{W}{A_1\rho_1 a_1} = 0.108$

Fig. 13 Axial Velocity Fluctuations Behind Inducer-Blade Row

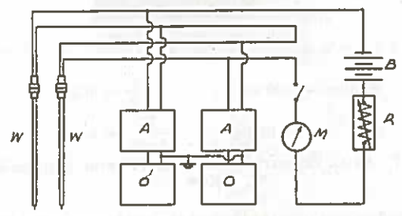

Fig. 14 Two-Channel Hot-Wire Instrument

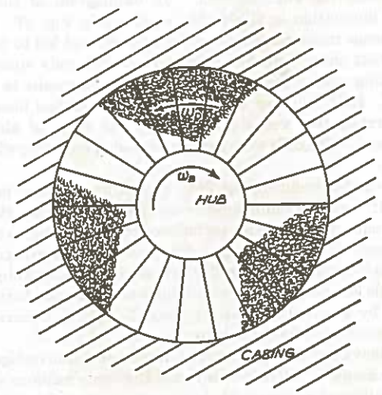

ω_B = velocity of blades relative to casing
ω_D = velocity of stall cells relative to blades

Fig. 15 Three-Cell Stall Pattern

When compressor flow was reduced slightly, the mild surge region was entered and the inducer behavior of Fig. 16 was observed. Prolonged bursts of blade stall were found to occur regularly at the previously recorded surge frequency of 10.5 cps. The oscillogram pattern represents a period of 16 consecutive wheel revolutions, or 1 surge cycle. Simultaneous hot-wire pictures showed that this surging was a universal behavior, the over-all flow changing from that corresponding to an incidence angle of 0 deg into stall and back again. As previously mentioned, this surge frequency did not depend on wheel speed. Note in Fig. 16 that during that part of the cycle in which flow is passing from good to bad, stall propagation is again in evidence.

Radius = 3.90 in. $\frac{U}{a_1} = 0.537$

$i = +8$ deg $\frac{W}{A_1\rho_1 a_1} = 0.100$

FIG. 16 AXIAL VELOCITY FLUCTUATIONS BEHIND INDUCER-BLADE ROW

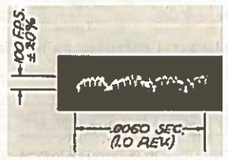

Radius = 3.90 in. $\frac{U}{a_1} = 0.537$

$i = +10$ deg $\frac{W}{A_1\rho_1 a_1} = 0.085$

FIG. 17 AXIAL VELOCITY FLUCTUATIONS BEHIND INDUCER-BLADE ROW

When flow was reduced beyond the mild surge point into the stable operating region between mild and deep surge, a third type of flow behavior was observed. An oscillogram of the axial-velocity fluctuation in this region is shown in Fig. 17. Again, simultaneous measurements were carried out and led to the conclusion that there were five cells of stall uniformly spaced and propagating around the wheel in the direction opposite to that of rotation. Each cell now involved about two stalled blades and had a propagation velocity relative to the rotor of about $^1/_4$ wheel speed. The cells were again wedge-shaped, being widest at the tip.

Upon further reducing the flow, erratic propagation patterns appeared; these were supplanted eventually by complete stall, the hot wire showing large-scale turbulence corresponding to separation in most of the exit passage. When the deep surge region was entered, a 9.5-cps pattern, similar to that of Fig. 16, was observed. Each cycle consists of a prolonged burst of large-scale turbulence followed by a period of relatively good flow; this behavior was simultaneous over the entire rotor.

The behavior of the single-stage compressor was investigated in a similar manner. Here it was found that only random stalling and unstalling of the rotor-blade tips occurred at the surge line. Also, it was found that a five-cell rotor-tip stall-propagation pattern rotating in a direction opposite to that of the wheel accounted for the predominant frequency previously recorded at lower flows. It was discovered, too, that in the so-called secondary-surge region rotor and stator were stall-propagating in unison, the pattern in this case being a single cell of stall extending about halfway around the periphery of the machine and extending from root to tip. This single cell also rotated in a direction opposite to that of the wheel; its frequency of appearance at a fixed position on the periphery was that of the previously observed secondary surge. The direct variation of this surge frequency with wheel speed was simply a manifestation of the dependency of propagation velocity on wheel speed. Then in fact there was no true over-all surge in the axial compressor studied. (This result should not be generalized since such surge might be expected in stages designed for more work.)

It thus appears that two distinct flow phenomena are responsible for observed compressor surge properties:

1 Helmholtz resonance type of system instability whose frequency is expected to be complexly dependent upon the characteristics of the compressor and its inlet and exit duct connections. A theoretical investigation of this over-all surge is presented in Section 3.

2 Stall propagation; a type of blade stall which affects groups of blades, which groups travel around the compressor row. The frequency in this case is proportional to the wheel speed. A theoretical investigation of this local stall type of surge is presented in Section 2. (It is hardly necessary to remark that these two types of instability will interact with one another; the general nature of this interaction will become clear in the sequel.)

2 STALL PROPAGATION

Introduction

As blade rows approach stall, the flow separates in some groups of blades and not in others. Such separated (stalled) regions follow one another around the wheel and are usually not stationary with respect to either the wheel or the case.

A qualitative explanation of this phenomenon is easy to give. Consider a cascade of airfoils operating on the verge of stall (large positive incidence angle) and suppose some transient disturbance causes one vane to stall momentarily (i.e., causes the vane boundary layer to separate on the convex side); then the flow area between that vane and the next is restricted momentarily. Since the cascade-exit pressure remains essentially constant (dependent on the mean turning through the whole blade row) the local flow must change, and, in fact, the result is a momentary choking of flow through the single blade passage. Flow ahead of the blade passage is diverted toward adjacent passages. The effect is to increase the angle of attack on the vane next in line in the direction of tangential component of inlet velocity and to decrease the angle of attack on the preceding vane, Fig. 18. Thus

FIG. 18 EFFECT OF STALLED VANE ON INLET FLOW

the next vane tends to stall and the preceding vane tends to become more stable. If the adversely affected vane does stall, it in turn affects the one next to it, and in this manner stall spreads along the blade row in the direction of inlet tangential velocity.

But when the stall has propagated some distance, the incidence angle on the first vane improves, because of the flow being diverted by the choking of succeeding blade passages, so that the first vane unstalls, and the unstalling process subsequently moves from blade to blade down the row. One might expect to find stall regions of a characteristic size propagating down the blade row with a velocity which depends upon the rate of formation and recovery of the separation regions.

The quantitative formulation of the problem involves several steps. By a small disturbance analysis, the condition for the appearance of large-scale disturbances can be obtained, and this is done. Following this, another analysis is required to determine the mean row characteristics observed during stall propagation; such an analysis would treat finite disturbances and would lead to the size of the separation region as well as to the resultant mean characteristics. Such a subsequent analysis is as yet not sufficiently useful to justify the labor involved.

Preliminary Definitions

Since the picture of the cause of stall propagation involves the changes of flow through a cascade under conditions of varying angle of attack, it is well to recast partly the customary cascade characteristics in a more appropriate form. The total-head profiles obtained behind a blade row usually are interpreted with the aid of a loss coefficient ζ defined by

$$\zeta = \frac{1}{A_x}\int_{A_x} \frac{p_{10} - p_{20}}{\frac{1}{2}\rho V_1^2}\, dA \qquad [1]$$

and of a pressure coefficient C_P defined by

$$C_P = \frac{1}{A_x}\int_{A_x} \frac{p_2 - p_1}{\frac{1}{2}\rho V_1^2} \qquad [2]$$

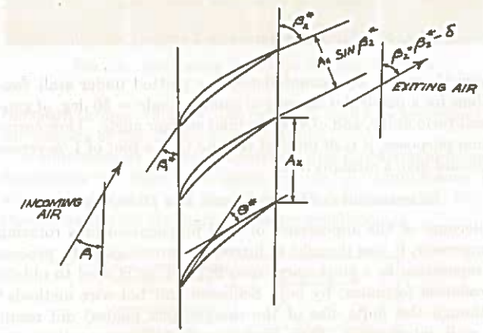

FIG. 19 FLOW THROUGH CASCADE

where the notation is as follows (see Fig. 19):

A_x = exit area of one flow passage

p_{10}, p_{20} = total head before and after cascade, respectively (measured in a reference system stationary with respect to the cascade)

p_1, p_2 = static pressure before and after cascade, respectively

ρ = density, assumed constant

V_1, V_2 = velocity before and after cascade, respectively

Let us define an effective flow area A_E as that area which would suffice to carry the entire exit flow if there were no losses. Thus if W is the flow rate

$$A_E = \frac{W}{[2\rho(p_{10} - p_2)]^{1/2}} = \int_{A_x}\left(\frac{p_{20} - p_2}{p_{10} - p_2}\right)^{1/2} \sin(\beta_2^* - \delta) \qquad [3]$$

where β_2^* is the angle of the trailing edges and δ the air-stream deviation, as shown in Fig. 19. Define next a flow coefficient α by

$$\alpha = \frac{A_E}{A_x \sin \beta_2^*} \qquad [4]$$

This quantity α will play a predominant role in the subsequent calculations; since most cascade correlations yield only ζ and C_P an approximate formula (assuming $\delta = 0$) relating α to these two quantities now will be derived.

Let $dx = dA/A_x$, so that x ranges from 0 to 1, and assume that the exit total pressure is that corresponding to a parabolic loss region of fractional extent y, i.e.

$$p_{20} = p_2 + \left(\frac{x}{y}\right)^2 (p_{10} - p_2) \text{ for } 0 < x < y$$

$$p_{20} = p_{10} \text{ for } y < x < 1$$

Then the equations for α and ζ yield

$$\alpha = 1 - \frac{1}{2}y, \quad \zeta = (1 - C_P)\frac{4y}{3}$$

whence

$$\alpha = 1 - \frac{3}{8}\left(\frac{\zeta}{1 - C_P}\right) \qquad [5]$$

Small Disturbance Analysis

Consider the flow of an incompressible fluid through a cascade

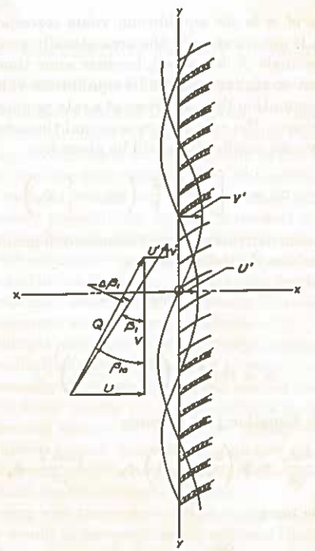

FIG. 20 DISTURBED FLOW THROUGH CASCADE

with an inlet velocity (far upstream) of magnitude Q and angle β_{10}. Fig. 20 shows the arrangement. The steady operation of the cascade will correspond to an inlet-flow angle of β_{10} and to a

flow-area coefficient of α_{00}. Suppose now that the flow is disturbed so that additional flow passes through certain sections and less through others. The disturbance velocities u' and v' are the derivatives of a disturbance velocity potential ϕ

$$\left.\begin{matrix} u' = \phi_x \\ v' = \phi_y \end{matrix}\right\} \phi_{xx} + \phi_{yy} = 0 \quad \ldots\ldots [6]$$

Separation of variables and use of the condition that $\phi \to 0$ as $x \to -\infty$ gives

$$\phi = \sum_1^\infty \left(a_n(t) \cos \frac{n\pi y}{b} + b_n(t) \sin \frac{n\pi y}{b} \right) e^{\frac{n\pi x}{b}} \quad \ldots\ldots [7]$$

where it is assumed that the disturbance is periodic in y. The values of $a_n(0)$ and $b_n(0)$ will depend on the initial shape of the disturbance; the manner in which a_n and b_n depend on t then will determine whether the disturbance grows or decays in time. The time dependence of the Fourier coefficients depends upon the cascade regarded as a boundary condition on the inlet flow. From Fig. 20

$$\tan \beta_1 = \frac{U + \phi_x}{V + \phi_y} \quad \ldots\ldots [8]$$

For purposes of stability analysis it is sufficient to assume a linear dependence between α_0 and $\tan \beta_1$, thus

$$\alpha_0 = \alpha_{00} + \left(\frac{d\alpha_0}{d(\tan \beta_1)}\bigg|_{\beta_1 = \beta_{10}} \right) \frac{\phi_x - \frac{U}{V}\phi_y}{V}$$

$$= \alpha_{00} + \alpha' \frac{\phi_x - \frac{U}{V}\phi_y}{V} \quad \ldots\ldots [9]$$

This value of α is the equilibrium value corresponding to u' and v' but it is not necessarily the area actually available at the time the flow angle β_1 is reached, because some time is required for the separation region to attain its equilibrium value. Making the simple assumption that A_E grows at a rate proportional to the difference between the equilibrium area and the actual area, the effective flow-area coefficient α will be given by

$$\frac{\partial \alpha}{\partial t} = \gamma(\alpha_0 - \alpha) = \gamma \left[\alpha_{00} + \frac{\alpha'}{V}\left(\phi_x - \frac{U}{V}\phi_y \right) - \alpha \right] \ldots [10]$$

where the partial derivative is used because α depends on y as well as on t. But from the definition of α

$$U + \phi_x = \omega\alpha$$

where

$$\omega = \sin \beta_2^* \cdot \left(\frac{2(p_{10} - p_2)}{\rho} \right)^{1/2}$$

and therefore Equation [10] becomes

$$\frac{\partial \phi_x}{\partial t} = \gamma \left(\frac{\omega\alpha'}{V} - 1 \right) \phi_x - \frac{\gamma\omega\alpha' U}{V^2}\phi_y$$

which has the form

$$\frac{\partial \phi_x}{\partial t} = B\phi_x - C\phi_y \quad \ldots\ldots [11]$$

This equation is the relation which must hold between the disturbance velocity components (ϕ_x, ϕ_y) at the cascade. It is essentially a boundary condition on the inlet-velocity distribution and serves to determine the Fourier coefficients of the inlet-disturbance velocities. Substitution of Equation [7] into Equation [11] then gives

$$\frac{da_n}{dt} = Ba_n - Cb_n$$

$$\frac{db_n}{dt} = Bb_n + Ca_n \quad \ldots\ldots [12]$$

The oscillatory solution of these equations grows or is damped according as $B > 0$ or $B < 0$, respectively, i.e., for instability

$$\alpha' > \frac{\alpha_{00}}{\tan \beta_{10}} \quad \ldots\ldots [13]$$

Geometrically, the flow is stable relative to propagation as long as the tangent to an α-tan β_1 characteristic cuts the α-axis above the origin. If the tangent were to cut the α-axis below the origin, then by the foregoing linearized theory all types of disturbances would be unstable. This leads us to expect that in general the tangent would pass approximately through the origin. That this expectation is borne out by experiment is indicated in Fig. 21,

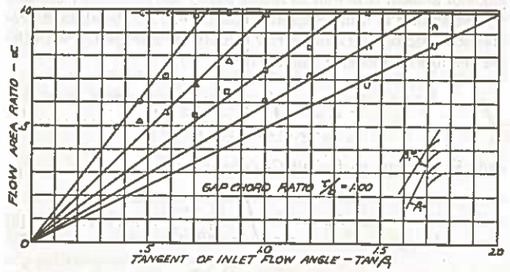

Fig. 21 Characteristics of Typical Cascade

where the α-tan β_1 characteristics are plotted under stall conditions for a particular cascade of camber angle = 50 deg, of gap-chord-ratio unity, and of varying inlet stagger angle. (For correlation purposes, it is of interest to note that a plot of $1/\alpha$ versus β_1 would give a straight line.)

Experimental Observations and Discussions

Because of the appearance of stall propagation in a rotating compressor, it was thought of interest to investigate the process of separation in a stationary cascade (such as is used to obtain correlation formulas) by both Schlieren and hot-wire methods.[8] Although the finite size of the cascade (six blades) did result in wall interference, very pronounced stall propagation was found.

Motion pictures of the stall behavior were taken, but unfortunately are not reproducible. Fig. 22 shows a sequence of Schlieren spark photographs arranged to simulate the motion-picture record. The motion pictures also disclosed an over-all surging of the mean through flow accompanying the stall propagation; this surging caused a periodic increase and decrease in the number of airfoils stalled and thereby served to obscure partially the propagation phenomenon.

At times it is difficult to determine from a Schlieren photograph whether an airfoil is stalled or merely passing to or from the stall condition. A better indication is given by a hot wire located so as to be in the wake region when a particular airfoil is stalled, but

[8] The experimental results described in this section are due to R. E. Kronauer.

in good flow when unstalled. By locating a second hot wire in a similar position at an adjacent airfoil, the velocity of stall propagation can be measured. Both this velocity and the angle of incidence at which intermittent stall first appears are functions of the mean through velocity; the results of such a measurement for the cascade of Fig. 22 are given in Table 1.

TABLE 1 STALL-PROPAGATION DATA FOR CASCADE OF FIG. 22

Upstream velocity, q_1, fps	No. of stalled airfoils in a typical propagating cell	Mean incidence deg	Propagating velocity, fps	Fraction of time a typical airfoil stalled
92		14.0	3–5	
		15.0	3–5	
288	3–4	14.5	17–21	0.4
		15.0	17–21	0.6
304	2–3 ½	14.5	13–18	0.4
		15.0	16–20	0.6
366	2–3 ½	14.5	23–27	0.5
		15.0	29–37	0.6
		13.5	43–51	0.3
466	2 ½–3 ½	14.0	43–51	0.6
		14.5	40–46	0.8
566	2 ½–3 ½	12.5	67–75	0.5
		13.0	50–75	0.7

Cascade characteristics:
$\beta_1^* = 70$ deg $\quad \theta^* = 30$ deg
$\beta_2^* = 100$ deg $\quad s/b = 0.67$

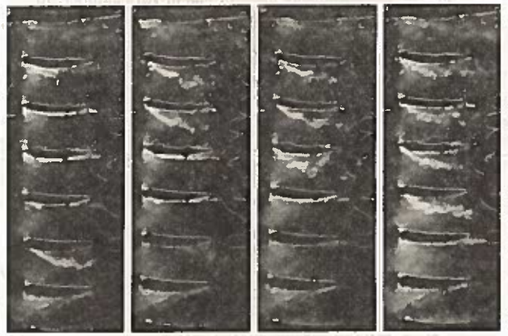

Fig. 22 Schlieren Views of Typical Cascade

A simultaneous record of upstream and downstream-velocity fluctuation (in time) was taken by use of simultaneous hot wires, one ahead of and the other behind the cascade. Fig. 23 shows clearly that the fluctuations are synchronized.

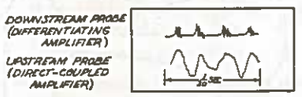

Fig. 23 Simultaneous Record of Upstream and Downstream Velocity Fluctuations in Cascade
Gain of direct-coupled amplifier is roughly 100 times gain of differentiating amplifier.)

Among the effects of stall propagation in a cascade tunnel is the excitation of the oscillation modes of the fluid in the ducting—an excitation which frequently prevents the taking of data at the bend of the loss curve.

From the solution for the velocity potential, it may be shown that the velocity of propagation of the disturbance is proportional to the wave length. This would imply that if an initial disturbance is of some arbitrary shape, this shape is not preserved during the subsequent propagation since the higher-harmonic components move more slowly. Since a fairly well-established pattern actually does occur, the finite amplitude disturbances are controlled by nonlinear effects.[9]

It may be noted that since the blade design varies spanwise in a typical blade row of an axial compressor, a portion (root or tip) of the blade will stall before the rest. The subsequent redistribution of flow then tends to inhibit stalling in the remainder of the span, thus sharpening the boundary between stalled and unstalled regions.

As the flow is decreased through a rotor, some point will attain the critical conditions for a sufficient time so that separation does occur. The diverted flow (diverted in all directions around the original spot) will cause (*a*) a sharpening of the spanwise edge of the separated spot, (*b*) a flow deterioration on the edge of the spot toward the convex side of the blades, and (*c*) a flow improvement on the edge of the spot toward the concave side of the blade. Because of the poor flow condition at the blade root and tip, one (or sometimes both) of these sections separates first. Thus propagating spots form and move around at the tip, for example, with a spanwise extension controlled primarily by the variation of cascade characteristics.

The actual flow through the compressor row, or cascade, consists of part good flow and part separated flow. The loss coefficients and pressure-rise coefficients in these two sections are different. If, however, we establish an operating point by, say, setting an inlet and exit pressure, this will determine the flow through the system and the fraction of the available area that is covered by the bad flow. While the analysis is not sufficiently complete to include in this paper it is important to note here that over-all conditions control the fraction of the area covered by separated spots while the interaction of the blades and inlet flow control their shape and propagation.

Considering the wide range of operation of a compressor, there is no hope of avoiding separation altogether. The only performance improvement that can be expected is to make the machine stall gracefully.

3 ELEMENTARY THEORY OF SURGE

Introduction and Experimental Background

In 1850, Helmholtz studied the behavior of "resonators," i.e., large jars with small necks, his assumption being that most of the kinetic energy of oscillation was to be found in the neck portion. He was able to show that the frequency of oscillation depended only on the enclosed volume and not on its shape, and that it was, in fact, inversely proportional to the square root of the volume. It was shown by later workers that a similar result held for the neck; i.e., the resonant frequency depended only on the area of the aperture and not on its shape. Various combinations of resonators and necks have been studied by people interested in acoustics; a good account may be found in reference (2).

About 1940 this phenomenon of organ-pipe resonance was used to give a qualitative picture of surging in water pumps (3) and recently essentially the same analysis was used to study nonlinear oscillations in water pumps (4). Both authors dealt with a system of reservoirs connected by narrow passageways some of which contained pumps possessing nonlinear characteristics. The analysis in each of these two cases was considerably simplified by the constant-density property of water.

When surging was encountered in air compressors, the Helmholtz theory would at first seem applicable and there is no doubt but that various attempts have been made to apply this theory to

[9] An entirely different approach, e.g., thin-wing theory, has been used by W. R. Sears. His analysis, while more complete in the inclusion of downstream effects, is less adequate in the inclusion of losses. The same propagation velocity and the same difficulties with nonlinear effects are encountered.

air-compressor surging (perhaps embodying an analysis similar to that to be discussed). However, no such analysis appears in the literature, possibly because of the fact that the predictions are apparently in error; the discrepancies disappear only when the presence of stall propagation is taken into account.

As mentioned in Part 1, it was discovered that the phenomenon previously called surge in the single-stage Harvard axial rig was not true surge, but consisted of a single-cell stall-propagation region trailing downstream from the rotor and rotating in time around the compressor axis. Because of this, it was decided to carry out all experimental surge work on the Harvard centrifugal compressor, where substantial and true surge does occur.

Two instruments were used to examine the static-pressure fluctuation in surge, the saran tubing—hot-wire arrangement of Part 1, and a steam-engine indicator-card apparatus. The former was used to measure the relative phases of the pressure fluctuations at different positions in the rig, and the latter to examine its shape and magnitude. An exhaustive series of tests were carried out, which for brevity will not be reported in detail, and the following results were obtained:

1 The maximum fluctuation in static pressure is of about the same order of magnitude as the maximum difference between inlet static and total pressure obtained in the normally operating compressor.

2 The wave form is approximately sinusoidal.

3 The fluctuations behind the rotor are almost in phase, e.g., the time-phase difference between the fluctuations at two different points behind the rotor is less than one fifth of the time required for a sound wave to pass between these two points. A similar result holds for the fluctuations ahead of the rotor; the fluctuations ahead of and behind the rotor are, however, not in phase. Fig. 24 gives a comparative survey of pressure patterns at various points in the rig, as obtained by use of a moving-film camera.

Station	Location
1	inlet chamber—60 in. ahead of rotor
2	inlet chamber—34 in. ahead of rotor
3	inlet nozzle—12 in. ahead of rotor
4	exit col. case—10 in. behind rotor
5	exit duct—60 in. behind rotor

FIG. 24 SIMULTANEOUS PRESSURE FLUCTUATIONS, CENTRIFUGAL RIG

These results imply that surging is a Helmholtz resonance effect and that it may be treated theoretically by using a linear small-oscillation theory (which always involves sinusoidal oscillations).

SURGE MODEL

Despite the simplicity of the following model, an analysis based on it turns out to predict fairly well the behavior of the centrifugal compressor.

Consider two chambers of volumes V_1 and V_2 connected to each other and to the atmosphere by means of three relatively narrow channels, the middle of which contains a compressor, as shown in Fig. 25. With reference to the figure, the nomenclature

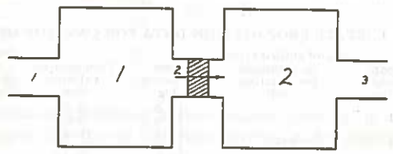

FIG. 25 SURGE MODEL

to be used is as follows:

V_i = volume of ith chamber, cu ft
p_i = instantaneous pressure in ith chamber, psf
p_0 = atmospheric pressure, psf
W_i = rate of mass flow in ith channel, lb per sec
M_i = instantaneous mass of gas in ith chamber, lb
T_i = instantaneous temperature of gas in ith chamber, deg F abs
$\rho_i = M_i/V_i$ lb per cu ft
g = acceleration of gravity, ft/sec²
R = gas constant $= \frac{V_i p_i}{M_i T_i}$, ft/deg $= C_p - C_v$
$P(W_2)$ = useful work per lb done by compressor (depends on W_2), ft
$P'(W_2) = dP/dW_2$
C_p = specific heat at constant pressure, ft/deg
C_v = specific heat at constant volume, ft/deg
$\dot{\phi} = d/dt(\phi)$, ϕ being any quantity
Q_i = channel constant, defined by Equation [14], ft/sec²/lb
κ = polytropic coefficient
γ = ratio of specific heats C_p/C_v

FLOW IN A CHANNEL

Consider a channel of variable cross-sectional area, as shown in Fig. 26. Let A be the area (sq ft) at a point x ft from the left-

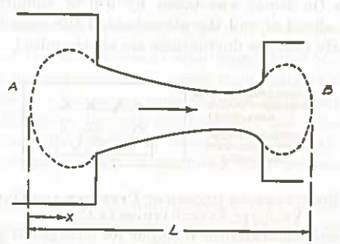

FIG. 26 CHANNEL SHAPE

hand end; let ρ be the instantaneous density (lb per cu ft) at this point. Then the total kinetic energy at any instant is

$$\frac{1}{2}\int_0^L \frac{W^2}{g\rho A}\,dx$$

where W is the mass-flow rate. Assume now that because of the small size of the channel the air in it moves almost as a "unit"; then W is constant and the instantaneous kinetic energy is

$$\frac{W^2}{2}\int_0^L \frac{dx}{g\rho A}$$

Define now the "channel constant" Q by

$$Q = \int_0^L \frac{dx}{g\rho A}$$

so that the kinetic energy is

$$\text{K.E.} = \frac{1}{2} QW^2 \text{ (lb-ft)} \quad \ldots\ldots\ldots\ldots [14]$$

In calculating the changes occurring in this quantity, it may be assumed that Q is constant in time, particularly since our interest is confined to the case of initial instability (at which time the oscillations are small). In the case of a channel linking two chambers of a compressor rig, the kinetic energy of the air is not confined to the channel region but extends somewhat outward from both ends, (Fig. 26). In calculating the channel constant for such a case, it will be assumed that the integration is carried out over that region occupied by appreciable kinetic energy.

BASIC EQUATIONS

If there is a compressor in the channel, then the rate of useful energy output of the compressor must equal the sum of the rate of increase of the foregoing kinetic energy and the rate at which energy is leaving the system. Using the notation of Fig. 26, where subscripts A and B refer to the conditions well ahead of and well behind the channel, i.e., to stagnation conditions, the energy equation applied to the system yields

$$WP(W) + WC_pT_A = WC_pT_B + Q\dot{W}W$$

which may be divided by W and differentiated to yield

$$P'(W)\dot{W} = C_p(\dot{T}_B - \dot{T}_A) + Q\ddot{W} \quad \ldots\ldots\ldots [15]$$

Assume now that the gas in the chamber obeys a polytropic relation of the form $p \sim \rho^\kappa$ (where κ is less than C_p/C_v because of the effect of dissipation, which is otherwise neglected). Then use of the gas law shows that

$$\dot{T} = (\kappa - 1)\frac{T}{M}\dot{M}$$

and Equation [15] then becomes

$$(P')\dot{W} = \frac{\gamma}{\gamma - 1}(\kappa - 1)R\left[\frac{T_B}{M_B}\dot{M}_B - \frac{T_A}{M_A}\dot{M}_A\right] + Q\ddot{W} \quad [16]$$

SOLUTIONS OF EQUATIONS

The result of writing Equation [16] for each of the three channels in Fig. 25 is (using $\dot{M}_1 = W_1 - W_2$, etc.)

$$Q_1\ddot{W}_1 + \gamma\frac{\kappa - 1}{\gamma - 1}R\frac{T_1}{M_1}(W_1 - W_2) = 0$$

$$Q_2\ddot{W}_2 - P'\dot{W}_2 + \gamma\frac{\kappa - 1}{\gamma - 1}R\left[\frac{T_2}{M_2}(W_2 - W_3) - \frac{T_1}{M_1}(W_1 - W_2)\right] = 0$$

$$Q_3\ddot{W}_3 - \gamma\frac{\kappa - 1}{\gamma - 1}R\frac{T_2}{M_2}(W_2 - W_3) = 0 \quad \ldots\ldots [17]$$

For small oscillations, P' may be assumed constant. It is a mathematical theorem that the solution of any such set of equations must have the form

$$W_i = C_i e^{\alpha t} \quad \ldots\ldots\ldots\ldots [18]$$

(or, more generally, the form of a polynomial in t multiplying $e^{\alpha t}$; such more general solutions exist only if the determinantal equation which shortly appears has multiple roots) and, therefore, we may substitute directly from Equation [18] into [17] to give

$$C_1\left[Q_1\alpha^2 + \gamma\frac{\kappa - 1}{\gamma - 1}R\frac{T_1}{M_1}\right] + C_2\left[-\gamma\frac{\kappa - 1}{\gamma - 1}R\frac{T_1}{M_1}\right] + C_3(0) = 0$$

$$C_1\left[-\gamma\frac{\kappa - 1}{\gamma - 1}R\frac{T_1}{M_1}\right] + C_2\left[Q_2\alpha^2 - P' \alpha + \gamma\frac{\kappa - 1}{\gamma - 1}R\left(\frac{T_2}{M_2} + \frac{T_1}{M_1}\right)\right] + C_3\left[-\gamma\frac{\kappa - 1}{\gamma - 1}R\frac{T_2}{M_2}\right] = 0$$

$$C_1(0) + C_2\left[-\gamma\frac{\kappa - 1}{\gamma - 1}R\frac{T_2}{M_2}\right] + C_3\left[Q_3\alpha^2 + \gamma\frac{\kappa - 1}{\gamma - 1}R\frac{T_2}{M_2}\right] = 0$$

For this set of equations to yield a set of nonsimultaneously vanishing C_i the determinant of the coefficients must vanish; after some simplification, this condition gives

$$\alpha\begin{vmatrix} Q_1\alpha^2 + \gamma\frac{\kappa - 1}{\gamma - 1}R\frac{T_1}{M_1} & Q_1\alpha & 0 \\ -\gamma\frac{\kappa - 1}{\gamma - 1}R\frac{T_1}{M_1} & Q_2\alpha - P' & -\gamma\frac{\kappa - 1}{\gamma - 1}R\frac{T_2}{M_2} \\ 0 & Q_3\alpha & Q_3\alpha^2 + \gamma\frac{\kappa - 1}{\gamma - 1}R\frac{T_2}{M_2} \end{vmatrix} = 0 \quad \ldots [19]$$

Now each root α of Equation [19] possesses, in general, a real and an imaginary part; if the real part is negative, the oscillation whose frequency is determined by the imaginary part will decrease in time, but if the real part is positive the oscillation will increase in time. The critical condition for instability, therefore, may be obtained by calculating that value of P' for which α has a zero real part. Setting $\alpha = i\omega$ and expanding Equation [19], we obtain a complex equation whose real and imaginary parts must vanish separately

$$\left(-\omega^2Q_1 + \gamma\frac{\kappa - 1}{\gamma - 1}R\frac{T_1}{M_1}\right)\left(-\omega^2Q_2 + \gamma\frac{\kappa - 1}{\gamma - 1}R\frac{T_2}{M_2}\right)P' = 0 \quad \ldots\ldots [20]$$

$$\left(-\omega^2Q_1 + \gamma\frac{\kappa - 1}{\gamma - 1}R\frac{T_1}{M_1}\right)\left(-\omega^2Q_2 + \gamma\frac{\kappa - 1}{\gamma - 1}R\frac{T_2}{M_2}\right)Q_2 + \left(\gamma\frac{\kappa - 1}{\gamma - 1}R\frac{T_1}{M_1}\right)\left(-\omega^2Q_2 + \gamma\frac{\kappa - 1}{\gamma - 1}R\frac{T_2}{M_2}\right)Q_1 + \left(\gamma\frac{\kappa - 1}{\gamma - 1}R\frac{T_2}{M_2}\right)\left(-\omega^2Q_1 + \gamma\frac{\kappa - 1}{\gamma - 1}R\frac{T_1}{M_1}\right)Q_3 = 0 \quad \ldots\ldots [21]$$

There are three factors in Equation [20]; if either of the first two factors vanishes, Equation [21], in general, cannot be satisfied. Hence $P' = 0$ is a requisite condition for (critical) instability. Equation [21] then determines the frequency. It is solved easily since it is a quadratic in ω^2

$$\left(\omega^2\frac{\gamma-1}{\gamma(\kappa-1)}\right)^2+\omega^2\frac{\gamma-1}{\gamma(\kappa-1)}\left[-R\left(\frac{T_2}{Q_2M_2}+\frac{T_1}{Q_1M_1}+\frac{T_1}{Q_2M_1}+\frac{T_2}{Q_2M_2}\right)\right]+R^2\frac{T_1}{M_1}\frac{T_2}{M_2}\left(\frac{Q_1+Q_2+Q_2}{Q_1Q_2Q_2}\right)=0\ldots[22]$$

To obtain an idea as to the order of magnitude of the various quantities involved, the following experimental results were obtained:

$Q_1 = 3.5$ sq ft per lb
$Q_2 = 1.6$ sq ft per lb
$Q_3 = 15$ sq ft per lb
$p_1 \cong p_0$
$p_2 \cong 1.2p_0$
$V_1 = 54$ cu ft
$V_2 = 4.4$ cu ft
$T_1 = 525$ F abs
$T_2 = 550$ F abs
Surge $f \cong 24$ cps

Then $RT_1/M_1 = 7500$, and $RT_2/M_2 = 82{,}500$; substitution into Equation [22] gives

$$\left(\omega^2\frac{\gamma-1}{\gamma(\kappa-1)}\right)^2-\omega^2\frac{\gamma-1}{\gamma(\kappa-1)}[5400+2100+4700+51{,}500]+147\times10^6=0\ldots.[23]$$

whence

$$f=\sqrt{\gamma\frac{\kappa-1}{\gamma-1}}\,(39.5)\text{ cps}$$

The value of κ is not known, but a good guess would be about 1.3. Then $f = 40$ cps; this is of the right order of magnitude when compared with the measured cycles per second but is somewhat too large. This is not unexpected, for the calculated value of each Q_i assumed that the kinetic energy was confined to the channel itself, whereas in practice it must extend considerably on both sides. This correction would decrease the calculated frequency, which is in the right direction. A much better check on the theory may be obtained by varying the exit volume. It will be noticed in Equation [23] that ω is dominated by the term $(RT_2)/(Q_2M_2)$; we therefore expect that if M_2 alone is varied, $\omega \sim 1/\sqrt{V_2}$. Experimentally, it was found that for $V_1 = \infty$, $V_2 = 4.4$ cu ft, f was 17.5 cps; for $V_1 = \infty$, $V_2 = 13.4$ cu ft, f was 9.5 cps. The two ratios are

$$\sqrt{\frac{4.4}{13.4}}=0.57 \qquad \frac{9.5}{17.5}=0.54$$

which agree rather well.

Knowing now the approximate relative magnitude of the quantities involved in Equation [22], an approximate expression for the frequency of pulsation may be obtained

$$f=\frac{1}{2\pi}\sqrt{\frac{\gamma(\kappa-1)}{\gamma-1}}\sqrt{\frac{RT_1}{M_1}\left(\frac{1}{Q_1}+\frac{1}{Q_2}\right)+\frac{RT_2}{M_2}\left(\frac{1}{Q_2}+\frac{1}{Q_3}\right)}\ldots.[24]$$

In an actual jet engine, volume 2 in Fig. 25 would represent the volume of the combustion chambers and the volume of the tubing between these and the compressor; volume 1 would represent the volume between the inlet-duct channel 1 and the compressor. The volume and shape of channel 2 would be that of the compressor passage. In general, the entrance to the compressor is practically atmospheric; this condition is equivalent to setting $M_1 = \infty$, and Equation [24] becomes

$$f=\frac{1}{2\pi}\sqrt{\gamma\frac{\kappa-1}{\gamma-1}\frac{RT_2}{M_2}\left(\frac{1}{Q_2}+\frac{1}{Q_3}\right)}\ldots\ldots.[25]$$

General Comments

Properties of Solution. It is essential, in using the model, that the entire impeller be considered as a unit. For example, if it were divided into its inducer-impeller components with a small intermediate volume, then the analysis would be erroneous because of the illegitimacy of the Helmholtz resonance assumption for so small a volume. For the same reason, all stages in a multistage compressor must be considered as lumped together if it is wished to apply the foregoing results. It is probable that this consideration is approximately valid in so far as a crude picture of over-all surge is concerned.

Because of the fact that $\alpha = 0$ is a root of Equation [19], another possible solution is $W_i = C_i' e^{0t} = C_i'$ (and by Equation [17] these C_i' must all be equal), and the general solution then is obtained by adding this constant solution to the previous oscillatory solution. In other words, the solution is valid if there is a steady air flow present, as of course there always is in practice. It also may be noted that if $P' = 0$, then $\alpha = 0$ is a multiple root, which corresponds to the case of a changing air flow. Thus, even in acceleration or deceleration, the condition $P' = 0$ must be satisfied for surging to occur, provided that the processes accompanying the change in speed are of a quasi-static nature.

The way in which the value of $(RT_2)/(Q_2M_2)$ dominates the frequency is probably worth emphasizing. Since changes in exit or entrance nozzle do not affect the value of this term, such changes would not be expected to alter the surge frequency by very much. Experiments in which a great many types of inlet and exit conditions were used (circular, elliptical, and multiple holes, bellmouth holes, pipes, and so on) bore out this expectation remarkably well.

The speed of the impeller does not enter directly into the expression for ω; it is, however, implicitly present in that the throttling condition for incipient pulsation will depend on the speed. But according to the previous remark, the change in throttling will have little effect and the change in frequency will depend on $(T_2/M_2)^{1/2}$ which would change but little, and hence it is expected that the frequency is relatively independent of speed. For small speed changes this is indeed the case.

Harvard Centrifugal and Axial Rigs. It should be noted that the condition for surge is that the slope of the useful-work-done per pound curve should vanish, not that the slope of the pressure-ratio curve should vanish. These two curves may be expected to have about the same shape for a moderately efficient compressor.

For the present centrifugal rig, the pressure-ratio curve shown in Fig. 27 indicates that the compressor should surge at point A.

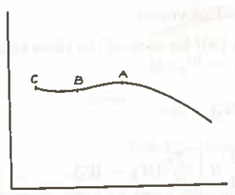

Fig. 27 Typical Centrifugal Characteristic

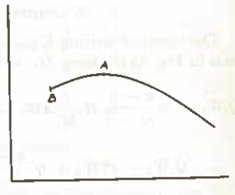

Fig. 28 Typical Axial Characteristic

This is indeed the case; further, because of the relatively gentle fall-off of the pressure-ratio curve, the pulsation is quite mild and is hardly detectable without instruments. When region B is reached, the operation is again stable; at point C the compressor drops into deep surge.

The pressure-ratio curve for the single-stage axial rig of Part 1 is reproduced in Fig. 28. Again, surge may be expected at point A, and, in fact, there is a sudden jump in the noise level at this point, corresponding probably to a rather high-frequency surge. The frequency of this surge may not be determined by the previous theory, because the dimensions are such that the frequency as calculated from Equation [22] is too high for the assumptions to remain valid. The theory, however, still may be expected to predict the point of incipience, as indeed it does, for the equations show that an instability of the Helmholtz type is possible, although once this instability occurs the dimensions are such as to force the resonance into a new pattern. As the flow is decreased, violent stall propagation sets in and dominates the rather weak surging.

BIBLIOGRAPHY

1 "Measurement of Instantaneous Vector Air Velocity by Hot-Wire Methods," by C. E. Pearson, *Journal of the Aeronautical Sciences*, vol. 19, February, 1952, pp. 73–82.
2 "Theory of Sound," by J. W. S. Rayleigh, Dover Publications, New York, N. Y., vol. 2, 1945, chapter 16.
3 "Untersuchungen an einer Kreiselpumpe mit labiler Kennlinie," by R. Dziallas, VDI-Verlag, Berlin, Germany, 1940.
4 "Stability and Surging of a Centrifugal Water Pump," by Sumiji Fujii, Transactions of the Society of Mechanical Engineers, Japan, vol. 13, no. 44, May, 1947, 1st report, pp. 184–191; 2nd report, pp. 192–201; and vol. 14, no. 48, 3rd report, pp. 12–17; 4th report, pp. 17–25. (in Japanese.)
5 "Compressor Surge Investigated by NACA," by R. O. Bullock and H. B. Finger, *SAE Journal*, vol. 59, September, 1951, pp. 42–45.

Discussion

W. R. Hawthorne,[10] M. D. Wood,[10] and J. H. Horlock.[10] Similar investigations to those described in the paper have been undertaken at the Cambridge University Engineering Laboratory, on an axial-flow compressor comprising three blade rows—guide vanes, rotor, and stator. The axial spacing of these rows may be varied.

These investigations, made with a hot-wire apparatus designed and built at Cambridge, have shown the existence of stalled cells of air rotating with the moving blades but with a slower angular velocity, confirming the results given by the authors.

The number and shape of these stalled patches vary not only with the mass-flow rate through the compressor but also with the axial spacing of the blade rows.

Completely different plots of total temperature rise and total pressure rise against mass flow are obtained with different axial spacing, and different stall patterns are observed. In all the compressor arrangements tested so far, the onset of stall-cell propagation on the rotating row is associated with a discontinuity in the total temperature rise-mass flow characteristic, whereas, as expected, initiation of propagation in a stator row has not been found to produce this effect.

It also has been noted that the start of rotating stall on the rotor tip may result in the unstalling of an adjacent downstream stator root. This is the reason for the differences in the over-all characteristics.

These results suggest that the effect of upstream and downstream adjacent blade rows must be included in any analysis if correct prediction of the velocity of propagation and dimensions of the stall cells in compressors are to be made theoretically.

M. C. Huppert.[11] This paper presents an interesting and timely account of surge and stall propagation. The authors were probably the first investigators to distinguish between surge and flow fluctuations due to stall propagation.

The writer's comments on the paper will serve largely to supplement the material presented. With regard to the analysis of surge, the authors neglected to include a throttle in the flow system for controlling the air flow. The inclusion of the compressor-discharge throttle complicates the criteria for stability so that $P' = 0$ is no longer the requisite condition for critical instability. In order to demonstrate the influence of the throttle, it will be convenient to resort to an electrical analogy of the flow system (see Olson[12] for a discussion of analogies between acoustical and electrical systems).

Set

$$C_i=\frac{\gamma-1}{\gamma(\kappa-1)}\frac{M_i}{RT_i}\text{ (capacitance)}$$

$$L_i = Q_i\text{ (inductance)}$$

$$I_i = W_i\text{ (current)}$$

$$E(I_2) = P(W_2)\text{ (electromotive force)}$$

For our purpose here, we will take

$$P(W_2)=\int_{p_{t_1}}^{p_{t_2}}\frac{dp_t}{\rho t}\cong\frac{p_{t_2}-p_{t_1}}{\rho t_{avg}}$$

An equivalent electric current for the system considered by the authors but with a throttle added is shown in Fig. 29, herewith.

The circuit element $E(I_2)$ represents the throttle and for steady flow the following conditions apply

$$I_1 = I_2 = I_3$$

$$E(I_2) = E(I_3)$$

By applying Kirchhoff's law to each of the three circuit loops shown in Fig. 29 and differentiating the resulting equations once with respect to time, the following expressions result

$$L_1\dot{I}_1+\frac{1}{C_1}(I_1-I_2)=0$$

$$L_2\dot{I}_2+\frac{1}{C_2}(I_2-I_3)+\frac{1}{C_1}(I_2-I_1)-[E(I_2)]'\dot{I}_2=0$$

$$L_3\dot{I}_3+\frac{1}{C_2}(I_3-I_2)+[E(I_3)]'\dot{I}_3=0$$

where

$$[E(I_2)]'=\frac{dE(I_2)}{dI_2}\text{ and }[E(I_3)]'=\frac{dE(I_3)}{dI_3}$$

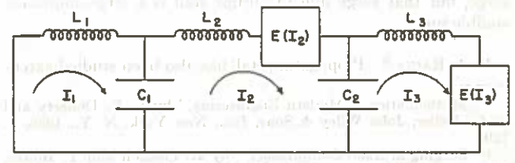

Fig. 29 Equivalent Electric Current for Surge Model

Following the same procedure used by the authors, we find an expression corresponding to Equation [19] but written as a polynomial in α as follows

[10] Cambridge University, Cambridge, England.
[11] National Advisory Committee for Aeronautics, Lewis Flight Propulsion Laboratory, Cleveland, Ohio.

[12] "Dynamical Analogies," by H. F. Olson, D. Van Nostrand Company, Inc., New York, N. Y., 1943.

$$\alpha^6 + (\tau_3 - \tau_2)\alpha^5 + (\Omega_1^2 + \Omega_2^2 + \Omega_3^2 + \Omega_4^2 - \tau_3\tau_2)\alpha^4 + [\tau_3(\Omega_1^2 + \Omega_2^2 + \Omega_3^2) - \tau_2(\Omega_4^2 + \Omega_1^2)]\alpha^3 + [\Omega_4^2\Omega_2^2 + \Omega_1^2\Omega_3^2 + \Omega_1^2\Omega_4^2 - \tau_2\tau_3\Omega_1^2]\alpha^2 + [\tau_3\Omega_1^2\Omega_2^2 - \tau_2\Omega_1^2\Omega_4^2]\alpha = 0$$

where $\tau_2 = \dfrac{[E(I_2)]'}{L_2}$ $\tau_3 = \dfrac{[E(I_3)]'}{L_3}$

$$\Omega_1^2 = \frac{1}{L_1C_1}, \quad \Omega_2^2 = \frac{1}{L_2C_2}, \quad \Omega_3^2 = \frac{1}{L_2C_1}, \quad \Omega_4^2 = \frac{1}{L_3C_2}$$

The necessary and sufficient condition for critical stability is given by Doherty and Keller,[13] as a system of relations among the coefficients in the foregoing expression.

If we consider the experimental values given by the authors, the following values are obtained

$\Omega_1^2 = 2000$ $\Omega_3^2 = 4700$
$\Omega_2^2 = 51{,}500$ $\Omega_4^2 = 5400$

The following table illustrates the effect of τ_3 on the value of τ_2 for critical stability

τ_3	τ_2 for critical stability
0	0 (authors' case)
60	5
600	10

Pearson[14] found that instabilities could occur at a compressor operating point with P' negative.

The fact that a compressor operating point is unstable does not mean that the resulting surge fluctuations will be sufficiently large to cause structural damage to the compressor. The nonlinear effects in the system will determine the amplitude of the surge fluctuations. If we assume that the major nonlinear effect is the variation of P with W_2, a distinction between two types of surge may be made. If the nonlinearity is progressive, that is, if P' changes gradually with W_2, the resulting surge fluctuations are analogous to feedback oscillations[15] and, if the nonlinearity is an essential nonlinearity such as a discontinuity in P, the resulting surge fluctuations would be analogous to relaxation oscillations. As pointed out elsewhere,[16] progressive nonlinearities in P at weight flows less than that for peak compressor-pressure ratio (where P' is positive) are probably due to a gradual or progressive stall of the compressor blading initiated by stall at one end of the blades, whereas essential nonlinearities or a discontinuity in P would likely be caused by abrupt stall.

The last reference[16] shows that a discontinuity in P is not sufficient to produce surge. The transient flow following abrupt stall must effect a stall recovery in order for surge to occur.

In general, NACA experience has been that surge resulting from progressive stall is a low-amplitude not easily detected surge, but that surge due to abrupt stall is a large-amplitude audible surge.

D. A. Rains.[17] Propagating stall has also been studied extensively at the California Institute of Technology[18] with results similar to those of the authors.

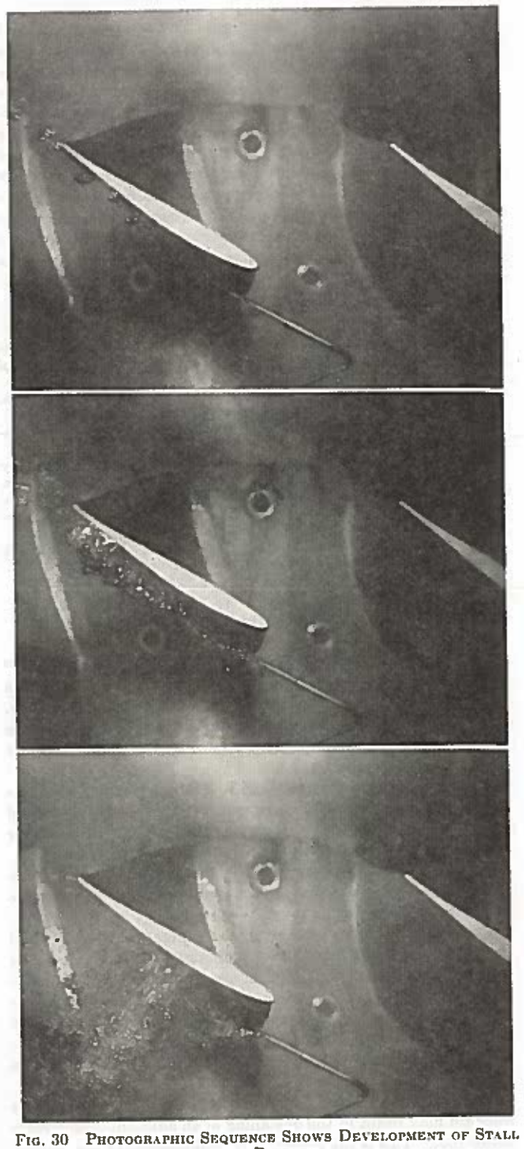

Fig. 30 Photographic Sequence Shows Development of Stall in a Passage

The recent construction of an axial-flow-pump test facility in the Hydrodynamics Laboratory has made possible the visual observation of stall. The pump is of compressorlike geometry and exhibits the same type of stalling phenomenon investigated by the authors. Visualization of the stall was accomplished by injecting

[13] "Mathematics of Modern Engineering," by R. E. Doherty and E. G. Keller, John Wiley & Sons, Inc., New York, N. Y., 1936, p. 129.

[14] "Surging in Axial Compressors," by H. Pearson and T. Bower, *The Aeronautical Quarterly*, published by the Royal Aeronautical Society, London, England, vol. 1, part 3, November, 1949.

[15] "Response of Physical Systems," by J. D. Trimmer, John Wiley & Sons, Inc., New York, N. Y., 1950.

[16] "Some Stall and Surge Phenomena in Axial-Flow Compressors," by M. C. Huppert and W. A. Benser, *Journal of the IAS*, December, 1953.

[17] Graduate Student, California Institute of Technology, Pasadena, Calif. Student Mem. ASME.

[18] "Experimental Investigations of Propagating Stall in Axial-Flow Compressors," by T. Iura and W. D. Rannie, Trans. ASME, vol. 76 1954, pp. 463–471.

air through a probe attached to the rotor and observing the flow patterns with a stroboscopic light through a window in the case of the pump. The sequence of photographs shown in Fig. 30 of this discussion was selected from a number of exposures taken at random times of the same blade passage. The figure shows the development of stall in a passage as the stall pattern travels around the blade row. These photographs confirm the scheme of propagating stall as proposed by the authors, Iura and Rannie,[18] and others.

Authors' Closure

As the jet engine has become better understood at its design point, more laboratories, industrial, governmental, and academic, have turned to a more detailed study of the problem of compressor surge which exerts such major influence on the starting and part-load characteristics of the engine. No laboratory gets very far before some aerodynamic observation or blade vibration (or breaking) study discloses the phenomena of stall propagation. Thus a large number of independent discoveries have resulted.

These have given rise to a number of independent theories as to the relation between various properties of the stall propagation and the relation between this and the general compressor-surge problem. Work on the mechanism of stall as reported by the discussers is essential if we are to attain a complete understanding of compressor performance. At present none of the theories—including that of the present authors—goes far enough to make stall-spot size, propagation velocity, or resultant compressor performance predictable from a given compressor geometry.

The interaction of adjacent blade rows as reported by Hawthorne, et al., from Cambridge University is indeed important, but the mechanism of this interaction is not clear.

The remarks of Huppert relative to the effect of the nozzle characteristic are correct, although analysis by electrical analogies does not seem necessary. Following the present work, which occurred some 2 years ago, a more detailed analysis of surge has been made by one of the authors (Pearson); the resultant formulation is much more complex and considers the effects of a variety of design parameters, including throttling conditions. This work has subsequently been submitted for publication.

The method of visualization reported by Rains is very interesting and should shed considerable light on the mechanism of stall which controls the compressor properties at low flows.